

UNIVERSITÀ DEGLI STUDI DI GENOVA
SCUOLA DI SCIENZE MEDICHE E FARMACEUTICHE
DIPARTIMENTO DI MEDICINA INTERNA E SPECIALITÀ MEDICHE



**DOTTORATO DI RICERCA IN EMATO
ONCOLOGIA E MEDICINA INTERNA CLINICO-
TRASLAZIONALE**

Ciclo XXXIII

**“ENDOTHELIAL SIRT6 BLUNTS STROKE SIZE
AND NEUROLOGICAL DEFICIT BY PRESERVING
BLOOD-BRAIN BARRIER INTEGRITY: A
TRANSLATIONAL STUDY”**

Relatore

Chiar.mo Prof. Fabrizio Montecucco

Correlatore

Chiar.mo Prof. Giovanni Guido Camici

Candidato

Dott. Luca Liberale

Anno Accademico 2019-2020

The herein reported PhD research project has reached its full development during the last year and was published in the form of an original research article in a peer-reviewed scientific journal.

*As such, this PhD thesis almost completely reproduces the relevant publication that can be found in Eur Heart J. 2020 Apr 21;41(16):1575-1587;
doi: 10.1093/eurheartj/ehz712.*

Reproduced by permission of Oxford University Press (<https://global.oup.com/>).

INDEX

INTRODUCTION	4
MATERIAL AND METHODS	6
RESULTS	17
DISCUSSION	23
CONCLUSIONS	28
TABLES AND FIGURES	29
REFERENCES	39
ACKNOWLEDGEMENTS	47

INTRODUCTION

Ischemic stroke is a major cause of mortality and morbidity worldwide whose prevalence is set to increase driven by the ongoing epidemiologic shift (1, 2). Yet, therapeutic strategies are limited to the early restoration of blood flow which can, on the other hand, worsen brain damage through ischemia/reperfusion (I/R) injury (3-5). Furthermore, due to the narrow treatment time window and the substantial number of contraindications only 1-2 out of 10 stroke patients are eligible for intravascular thrombolysis (6, 7). Safe and effective approaches to contain cerebral ischemic damage are long-term unmet medical needs and a better understanding of stroke pathophysiology is essential to identify novel molecular target to widen our interventional options in this setting.

Standing at the interface between cerebral circulation and the brain parenchyma, the blood-brain barrier (BBB) regulates diffusion of solutes and protects the brain from circulating pathogens (8). Together with pericytes and astrocytes, cerebral microvascular endothelial cells critically control BBB permeability through the expression of different tight- and adherens-junctions (8). Following an ischemic stroke, I/R-mediated BBB disruption associates with vascular leakage and infiltration of circulating cells and solutes leading to edema and worsened parenchymal damage (3, 5, 8, 9). Accordingly, in ischemic stroke patients barrier impairment is associated with haemorrhagic transformation and worsened outcome (10-12) thus indicating BBB as a promising therapeutic target to blunt I/R-mediated cerebral injury.

Aging is a major risk factor for stroke and several genes regulating lifespan were shown to determine cerebral damage in I/R brain injury (1, 13, 14). Specifically, members of the sirtuin (SIRT) superfamily play an important role in regulating

biological processes such as aging, cell metabolism, redox balance, inflammation and apoptosis which are key to the pathophysiology of stroke (15, 16). SIRT6 is a involved in telomere/genome stabilization, DNA repair but also inflammation and glucose or fat homeostasis (17). Furthermore, SIRT6 is a well-recognized longevity gene where *Sirt6* transgenic mice were shown to have an increased life span compared with wild-type controls (17). Through its negative regulator function on myocardial IGF-Akt signaling, *Sirt6* deficiency results in cardiac hypertrophy and heart failure whereas SIRT6 overexpression increases hypoxia resistance in cardiomyocytes (17). The role of SIRT6 in brain disease has been inconclusively explored (18); indeed so far, a possible protective role has been suggested only for neuronal SIRT6 in a preclinical study (19).

Given the pivotal role of endothelial cells in BBB function and the prognostic relevance of BBB damage in stroke patients, we hypothesized that the endothelial-specific expression of the longevity gene *SIRT6* may be protective in the setting of ischemic stroke. Accordingly, in this study we investigated whether specific deletion of endothelial *Sirt6* affects cerebral damage in a mouse model of stroke. Also, we tested SIRT6 as a potential therapeutic target by post-ischemically inducing its expression in mice so as to mimic a clinically relevant experimental setup. Furthermore, to increase the translational relevance of our data, we assessed the relevance of SIRT6 in the barrier function using primary human brain microvascular endothelial cells (HBMVECs) exposed to hypoxia/reoxygenation. Finally, we assessed *SIRT6* expression in ischemic stroke patients and correlated it to outcome as assessed by the National Institute of Health Stroke Scale (NIHSS).

MATERIAL AND METHODS

Animals

All mice were kept in a temperature-controlled animal facility under normal light/dark cycle with free access to food and water for the whole duration of the experiments herein described. All procedures were approved by the Committee for Animal Testing of the Canton of Zurich, Switzerland (license n. ZH114/18). Animal experiments were performed conform to the Directive 2010/63/EU of the European Parliament and of the Council of 22 September 2010 on the protection of animals used for scientific purposes. Animal experiments were reported according to Animal Research: Reporting in Vivo Experiments (ARRIVE) guidelines.

Endothelial-specific *Sirt6* knock-out mice

Animal experiments were performed on 12-week-old endothelial-specific homozygous *Sirt6* knockout (*eSirt6*^{-/-}) male mice and age-matched *Sirt6* floxed littermates (*Sirt6*^{fl/fl}). Both groups were maintained on C57BL/6 background. *eSirt6*^{-/-} mice were generated by crossbreeding *Sirt6*^{fl/fl} mice with hemizygous mice overexpressing Cre-recombinase under control of vascular endothelial-specific cadherine (*Cdh5*) promoter (*Cdh5-Cre*^{Tg/+}). The presence of the *Sirt6* floxed and excised knockout allele as well as of Cre recombinase was confirmed by routine genomic PCR using following PCR primers: for *Sirt6* floxed: 5'- AAC TGA CTG TTG CGG CAG AG-3' forward, 5'-CCT GTC CCA TTC TGA GGA C-3' reverse; for *Sirt6* knockout: 5'- AAC TGA CTG TTG CGG CAG AG-3' forward, 5'-GCT GGG ATT AAA GGC TGC G-3'; for *Cre*: 5'-AAC TGA CTG TTG CGG CAG AG-3' forward, 5'-CCT GTC CCA TTC TGA GGA AC-3'

reverse. PCR products were visualized on either 4% (*Sirt6*) or 1.5% (*Cre*) agarose gel.

Post-ischemic *Sirt6* overexpression

12-week-old C57BL/6 wild-type males treated with either cloning vector (pCMV) or *Sirt6* cDNA clone (*Sirt6*) were used for post-ischemic *Sirt6* overexpression experiments. Briefly, after 45 mins of ischemia and upon retraction of the occlusive filament (beginning of reperfusion) animals were randomly injected i.v. either with 40µg of cloning vector (Origene, PCMV6-Entry, PS100001) or a predesigned mouse *Sirt6* cDNA clone (Origene, MC200652) together with a cationic transfection reagent jetPEI® (Polyplus Transfection™, New York, NY, USA), according to the manufacturer's instructions (<http://www.polyplus-transfection.com>), as previously described (20). In pilot experiments exploring the temporal dynamic of cDNA delivery, mice did not undergo transient middle cerebral artery (MCA) occlusion (tMCAO). Euthanasia was induced with carbon dioxide at different time-points after plasmid injection. Then, the animal was perfused with 10 mL cold PBS before harvesting vessels. Common carotid artery and MCA were identified using a dissecting microscope and excised in total.

Isolation of endothelial cells

Mice were perfused with PBS through the left ventricle; lung tissue, excluding central bronchi, was collected and minced with surgical blades. Then, it was incubated for one hour at 37 °C, under continuous agitation in a solution containing collagenase type 2 and dispase (Invitrogen). Digests were then passed through a 100 µm strainer and centrifuged at 400g. To remove red blood cells, granulocytes, non-vital cells and cell debris, cells were re-suspended in Ficoll

separation medium, and the suspension was carefully layered on Ficoll-Paque (Amersham) and spun 400g for 20 min at 18°C without brakes. The interphase containing viable cells was then transferred into a fresh tube containing EC isolation medium. Finally, cells were sorted by using an anti-mouse CD31 MicroBeads (Miltenyi Biotec) (21).

Transient middle cerebral artery occlusion

To induce I/R brain injury, tMCAO was performed as previously described (22, 23). Briefly, mice were anaesthetized using isoflurane 3 % and 1.5 % for induction and maintenance respectively, while body temperature was kept at 37°C. For analgesia, 0.5% bupivacaine was infiltrated at the incision side. Ischemia was induced by inserting a 6-0 silicone-coated filament (Doccol Corporation, Sharon, MA, USA) into the common carotid artery until the origin of the left MCA after the dissection of common, internal and external carotid arteries. After 45 minutes, reperfusion was allowed for 48 h before animal euthanasia with carbon dioxide. After euthanasia, peripheral blood was collected by intracardial puncture. Then, the animal was perfused with 10 mL cold PBS before harvesting brain and vessels. MCA origin was identified using a dissecting microscope and excised in total. The well-being of mice during the experimental period was determined using a score sheet that was approved by the Cantonal Veterinary Office of the Canton of Zurich. This score sheet was used to define survival/death of an animal. Death events include spontaneous deaths (1 of 17 for *Sirt6^{fl/fl}* and 7 of 22 for *eSirt6^{-/-}*) and mice which did not fulfil the health evaluation criteria.

Stroke volume

For determination of stroke volumes, murine brains were cut into 5 (2-mm thick) coronal sections and immersed in a 2% solution of 2,3,5-triphenyltetrazolium chloride (TTC) (Sigma-Aldrich, Chemie GmbH, Buchs, Switzerland) at 37°C for 20 min. Stroke areas, were quantified using ImageJ Software (Image J, NIH, MD, USA). The following formula was applied in order to compensate for cerebral swelling (edema) and subsequent overestimation of the infarct volume as previously described (16): corrected infarct volume = contralateral hemisphere volume - (ipsilateral hemisphere volume - infarct volume).

Neurological deficit assessment

Neurological status was assessed 2, 24 and 48 h after tMCAO by a four-point scale neurological score based on Bederson et al. (24) as follows: grade 0, normal neurological function; grade 1, forelimb and torso flexion to the contralateral side upon lifting the animal by the tail; grade 2, circling to the contralateral side; grade 3, leaning to the contralateral side at rest; grade 4, no spontaneous motor activity, as previously described (25). Neurological performance was determined by the RotaRod test: animals were placed on a rotating rod at increasing speeds (4–44 revolutions/min) and latency to fall was recorded (26).

Immunohistology

Immunohistological stainings of infarcted brains were performed as previously described (16). Briefly, following induction of deep anesthesia, mice were transcardially perfused with phosphate buffered saline (PBS) (Sigma-Aldrich, Chemie GmbH, Buchs, Switzerland). The brains were removed and consecutively incubated overnight in 4.0% PFA at 4 °C and afterwards transferred to 30% sucrose in PBS for 36 h. Cryoprotected brains were cut into 100-µm thick free-

floating sections pre-treated with proteinase K for antigen retrieval and immune-blocked. After these, sections were incubated with primary antibodies at the following dilution: the endothelial marker CD31 (550274; 1:50; BD Pharmingen, Allschwil, Switzerland), SIRT6 (#12486S; 1:50; Cell Signalling Technology, Danvers, MA, USA) and cleaved caspase-3 (#9664S; 1:400; Cell Signalling) at 4°C overnight, respectively. After washing, brain sections were incubated with the appropriate secondary antibodies (Jackson ImmunoResearch, West Grove, PA, USA) for 24 h at room temperature. Images were acquired using a confocal microscope (Leica SP8; Leica, Wetzlar, Germany). Stained area of Sirt6 and cleaved caspase-3 was measured using ImageJ Software and normalized to the total endothelial cell surface assessed by CD31 staining.

BBB permeability was measured assessing endogenous immunoglobulin G (IgG) extravasation, sections were blocked for 60 min followed by incubation with Alexa647-conjugated donkey anti-mouse IgG for 24 h (715-605-151; 1:600; Jackson ImmunoResearch, West Grove, USA). IgG leakage was corrected for edema, as previously described in stroke volume assessment, and expressed as a percentage of the total contralateral hemisphere volume.

Cell culture experiments

Primary human brain microvascular endothelial cells (HBMVECs) (Cell Systems, Kirkland, WA, USA) between passages 6 and 8 were used for *in vitro* experiments. Endothelial cells were cultured in Endothelial Cell Growth Medium (Cell Applications Inc., San Diego, CA, USA), supplemented with and 10% fetal bovine serum (BSA, Thermo Fisher Scientific, Waltham, MA, USA). Cells were grown to 80 % confluence before being transfected with *SIRT6* small interfering RNA (si*SIRT6*; Santa Cruz, Dallas, TX, USA) or scramble siRNA (siSCR;

Microsynth, Balgach, Switzerland) for 24 h using the Lipofectamine® 3000 transfection kit according to manufacturer's recommendations (Invitrogen, Carlsbad, CA, USA). Next, cells were exposed to hypoxia (0.2% oxygen) for 4 h followed by 4 h of normoxia (21% oxygen) (reoxygenation) or kept at normoxic conditions (21% oxygen) for 8 h, as previously shown (27). Hypoxia was induced using a gas-controlled glove hypoxia workstation (Invivo₂ 400, Baker Ruskinn, Sanford, ME, USA).

Measurement of Barrier Function by Transendothelial Electrical Resistance

Measurements of transendothelial electrical resistance (TEER) on HBMVEC monolayers were performed using the electric cell-substrate impedance system (ECIS) Z Theta system (Applied Biophysics, Troy, NY, USA) as previously described (16). The ECIS system provides real-time monitoring of changes in TEER. In brief, HBMVECs at 9×10^5 /well were plated on fibronectin coated 8W10E+ electrode arrays (Applied Biophysics). Then, cells were allowed to form monolayers until stable TEER values were reached. After 5 h, the monolayers were treated with *SIRT6* or scramble siRNA as previously specified. Then, they were exposed to hypoxic conditions for 4 h followed by reoxygenation for 48 h. Measurements were conducted at multiple frequencies ranging from 62.6 Hz to 64 kHz. Data were expressed as TEER percent change from baseline values (average of last 3 measurements before hypoxia).

Western blotting

Protein expression was determined by Western blot analysis. Murine vessels and endothelial cells were lysed (Tris 50 mM, NaCl 150 mM, EDTA 1 mM, NaF 1 mM, DTT 1 mM, aprotinin 10 mg/mL, leupeptin 10 mg/mL, Na₃VO₄ 0.1 mM,

phenylmethylsulfonyl fluoride (PMSF) 1 mM, and NP-40 0.5%) and total protein concentration was determined according to the manufacturer's recommendations (Bio-Rad Laboratores AG, Fribourg, Switzerland); 20 – 30 µg of total protein lysates were separated on an 8 or 10% SDS–PAGE before being transferred to a polyvinylidene fluoride membrane by wet transfer (Bio-Rad Laboratores AG, Fribourg, Switzerland). Membranes were incubated with primary antibodies against SIRT6 (#12486S; 1:1000; Cell Signalling), cleaved caspase-3 (#9661S; 1:1000; Cell Signalling), phospho-Akt (#4060S; 1:1000, Cell Signaling), Akt (#9272S; 1:1000, Cell Signaling) and glyceraldehyde 3-phosphate dehydrogenase (GAPDH) (MAB374; 1:40000; Merck Millipore, Billerica, MA, USA) over night at 4°C on a shaker. Secondary antibodies anti-mouse (1031-05) and anti-rabbit (4050-05) were obtained from Southern Biotechnology (Birmingham, AL, USA) and applied for 1 h at room temperature. Densitometric analyses were performed (Amersham Imager 600, General Electric; Healthcare Europe GmbH, Glattbrugg, Switzerland) and protein expression was normalized to GAPDH (SIRT6 and cleaved caspase 3) or total Akt (phospho-Akt).

Cytotoxicity Detection

Lactate dehydrogenase (LDH) release was determined in supernatant from cultured HBMVECs according to manufacturer's recommendations (Cytotoxicity Detection Kit; Roche, Basel, Switzerland). Briefly, enzymatic activity of cytoplasmic LDH released from dead cells was detected by conversion of NAD⁺ to NADH/H⁺ and subsequent reduction of Iodotetrazolium chloride to formazan (red). Absorbance was determined at 490 nm using an enzyme-linked immunosorbent assay (ELISA) plate reader (Infinite M200 pro; Tecan Group Ltd., Männedorf, Switzerland).

Co-immunoprecipitation

Endothelial cell lysates were centrifuged at 10,000 g to remove insoluble material. For immunoprecipitation, precleared lysates were incubated with Akt antibody overnight at 4°C. Lysates were precleared by incubation with 50 µL of protein A/G-agarose for 4 h at 4°C with rocking. Agarose beads were pelleted by centrifugation at 1000 g. Immunoprecipitated proteins were eluted from the beads by boiling for 5 min in SDS sample buffer and immunoblotted with primary antibodies against Akt (1:1000) and SIRT6 (1:1000). Bound antibody was visualized using an enhanced chemiluminescence system (Merck Millipore, Billerica, MA, USA) after incubation with peroxidase-conjugated secondary antibody for 1 h.

Patients

Ischemic stroke patients (n=14) admitted to the emergency room of San Raffaele Hospital (OSR, Milan, Italy) within 6 h after symptom onset were enrolled in the present study. Patients diagnosed with diabetes, systemic inflammatory diseases, acute infections, and active malignancy were excluded to eliminate potential interference of those disease states on SIRT6 expression. Venous blood was collected 24 h after initial stroke symptoms. Of the 14 ischemic stroke patients, 5 received intravascular thrombolytic treatment with recombinant tissue plasminogen activator within 4.5 h from initial symptom onset. Ischemic strokes were diagnosed based on clinical history, neurological examination and a brain computed tomography scan at arrival in the emergency department; stroke aetiology was defined according to the Trial of ORG 10172 in Acute Stroke Treatment (TOAST) criteria (28). MCA occlusion was defined according to the presence of hyperdense artery sign on non-contrast CT scan (29). Ischemic

volume was measured at follow-up non-contrast CT scan by using the formula $ABC/2$ according to an ellipsoid model (A: longest dimension in axis x, B: longest perpendicular dimension to axis x (y), C: total length in z dimension) (30). Stroke severity was assessed using NIHSS on hospital admission and at discharge. Furthermore, $\Delta\text{NIHSS}\%$ was calculated as the difference between the NIHSS presented at discharge and the NIHSS presented at admission relativized on initial NIHSS [$\Delta\text{NIHSS} = (\text{NIHSS discharge} - \text{NIHSS admission}) / \text{NIHSS admission}$]; thereby, positive values indicate short-term neurologic worsening while negative values indicate neurological improvement. The study was approved by the local Ethics Committee at San Raffaele Scientific Institute, Milan, Italy and was performed conform to the declaration of Helsinki. All participants (or their representative relatives) provided signed informed consent.

Isolation of peripheral monocytes from study subjects

Monocytes from whole blood were isolated using anti-CD14-coated MicroBeads (Miltenyi Biotec, Bergisch Gladbach, Germany) on a magnetic separator (Miltenyi Biotec, Bergisch Gladbach, Germany), as previously described (31).

Real-time PCR

Real-time PCR have been applied to assess gene expression in patients' monocytes as previously described (27). Total RNA was extracted from patients' monocytes using TRI Reagent (Merck KGaA, Darmstadt, Germany) according to the manufacturer's recommendations. Conversion of the total cellular RNA to cDNA was performed with Moloney murine leukemia virus reverse transcriptase and random hexamers (GE Healthcare, Little Chalfont, UK) in a final volume of 35 μl , using 2 μg of total RNA according to manufacturer's recommendations.

RT-PCR was performed in a QuantStudio 7 Flex RT-PCR cycler (Applied Biosystems, Foster City, CA, USA) according to the manufacturer's instructions. All RT-PCR experiments were performed using the SYBR Select Master Mix provided by Applied Biosystems (Life Technologies, Carlsbad, CA, USA). Each reaction (20 μ l) contained 2 μ l cDNA, 400 fmol of each primer and 10 μ l of Master Mix. The following primers were used (all from Microsynth): for h*SIRT6*: forward 5'-GCT TCC TGG TCA GCC AGA-3', reverse 5'-CTT GGC ACA TTC TTC CAC AA-3'; for actin β (h*ACTB*): forward: 5'-GCA CAG AGC CTC GCC TT-3' and reverse: 5'-GTT GTC GAC GAC GAG CG-3'. The amplification program consisted of 1 cycle at 95°C for 10 min, followed by 40 cycles with a denaturing phase at 95°C for 15 s, an annealing/elongation phase at 60°C for 1 min. A melting curve analysis was performed after amplification to verify the accuracy of the amplicon. Cycle threshold (C_t) values for each gene were obtained for each sample and analysed with Graph Pad Prism 6 software (GraphPad Software, Inc, La Jolla, CA, USA). Differences in C_T values (ΔC_T) between the test gene and the endogenous housekeeping control (h*ACTB*) were calculated and used for statistical analyses.

Statistical analysis

Data are expressed as mean \pm standard deviation (SD). All statistical analyses were performed using GraphPad Prism 6 software (GraphPad Software, Inc, La Jolla, CA, USA). Data were analysed by using unpaired two-tailed Student's t-test to compare two independent groups, Cohen's d was calculated as measure of the effect size and expressed as d and 95% (confidence interval) CI (32). For repeated measurements, two-way ANOVA with Sidak *post hoc* test was used. Fisher's exact test was used for comparison of categorical data between study subjects and

Pearson's correlation analysis was used to test the correlation between two quantitative variables. Statistical analysis for survival studies was performed using log-rank (Mantel-Cox) test. A probability value (P) below or equal 0.05 was considered as statistically significant.

RESULTS

Generation of the endothelial-specific *Sirt6* knockout mice

Endothelial-specific *Sirt6* homozygous knockout mice were generated by crossbreeding *Sirt6^{fl/fl}* mice with hemizygous mice overexpressing Cre-recombinase under control of vascular endothelial-specific cadherine (*Cdh5*) promoter (*Cdh5-Cre^{Tg/+}*)(Fig. 1A). In the resulting *Sirt6^{fl/fl} Cdh5-Cre^{Tg/+}* double mutant animals, the *Sirt6* sequence flanked by two loxP sites is excised by Cre-mediated recombination in the endothelium thus leading to selective deletion of *Sirt6*. The endothelium-specific removal of the flanked region was confirmed on isolated murine endothelial cells by genomic PCR using *Sirt6*- and *Cre*-specific primers (Fig. 1B). At the time of experiment, *eSirt6^{-/-}* and *Sirt6^{fl/fl}* littermates did not show any difference in terms of blood pressure and fasting lipid or glucose levels (data not shown).

Brain ischemia/reperfusion reduces endothelial SIRT6 expression in cerebral vessels

To test the responsiveness of vascular SIRT6 to stroke *in vivo*, tMCAO was performed in *SIRT6^{fl/fl}* mice for 45 minutes followed by 48 h of reperfusion. Next, endothelial SIRT6 expression after stroke was assessed by co-staining SIRT6 with CD31 - an endothelial specific protein - in the infarcted penumbra area and compared to that of the unaffected contralateral hemisphere. I/R injury strongly reduced expression of SIRT6 in vessels from the ipsilateral hemisphere, as compared to those located in the contralateral one ($d=1.04$ (95%CI 0.04-2.04); $P=0.016$, Fig. 2A).

Endothelial-specific *Sirt6* deletion worsens ischemia/reperfusion-induced cerebral damage and post-stroke outcome in mice.

To evaluate the relevance of endothelial *Sirt6* in cerebral I/R injury, *eSirt6*^{-/-} mice underwent tMCAO. Following 45 minutes of ischemia and 48 h of reperfusion (Fig. 2B) *eSirt6*^{-/-} mice revealed increased infarct volumes compared to control animals, as assessed by TTC staining ($d=1.75$ (95%CI 0.68-2.81); $P=0.005$; Fig. 2C). Accordingly, survival 48 h after tMCAO was significantly reduced in *eSirt6*^{-/-} as compared to *Sirt6*^{fl/fl} littermates (68% vs. 94%, $P=0.046$; Fig. 2D). Also, post-stroke neurological deficits have been quantified by two different tests at different time-points. At baseline, *eSirt6*^{-/-} mice and *Sirt6*^{fl/fl} littermates showed no differences in terms of neurological- and motor-function, as assessed by RotaRod test and Bederson-based neurological index (Fig. 2E and 2F). 24 h and 48 h after stroke, *eSirt6*^{-/-} mice displayed a significantly shorter latency to fall from the rotating rod compared to *Sirt6*^{fl/fl} animals, indicating a greater impairment of motor function ($P=0.004$ and $P=0.010$, respectively; Fig. 2E). In line with this, also the neurological deficits according to the Bederson-based scale were significantly worsened in *eSirt6*^{-/-} mice than in control littermates at both 24 and 48 h after the experiment ($P=0.001$ and $P<0.0001$, respectively; Fig. 2F).

Post-ischemic *Sirt6* overexpression reduces ischemia/reperfusion-induced cerebral damage

To test the potential of SIRT6 as a therapeutic target in the setting of ischemic stroke, we induced *Sirt6* overexpression in WT mice. In vivo overexpression of SIRT6 was performed by intravenous injection of a predesigned cDNA clone (*Sirt6*) together with a cation transfection reagent. Already 24 h after the injection the expression of *Sirt6* in the carotid artery was increased by 3 fold and lasted for

at least 96 h, as compared to control animals receiving cloning control vector (pCMV) (Fig. 3A).

In order to reproduce a clinically relevant experimental setup, *Sirt6* overexpressing clone was injected after the ischemic event, upon reperfusion thus mimicking the situation of patients presenting to the emergency care unit with ischemic stroke and eligible for thrombolytic therapy (Fig. 3B). Despite the post-ischemic treatment, SIRT6 overexpression led to a drastic reduction in stroke size of more than 50% at 48 h after tMCAO ($d=4.18$ (95%CI 2.96-5.40); $P<0.0001$; Fig. 3C). Accordingly, post-ischemic *Sirt6* overexpression also blunted neurological impairment at 24 and 48 h of reperfusion as assessed by both RotaRod test and Bederson index ($P=0.010$ and $P=0.016$ for RotaRod test and $P=0.042$ and $P=0.007$ for Bederson index; Fig. 3D and 3E, respectively).

The successful cDNA delivery have been confirmed also in MCA lysates (Fig.4)

Endothelial-specific *Sirt6* deletion increases BBB disruption and caspase 3 activation.

To assess BBB impairment, IgG immunohistochemistry was performed on brain sections. Both *eSirt6*^{-/-} and *Sirt6*^{fl/fl} animals showed IgG leakage in the ipsilateral hemisphere 48 h after tMCAO, whereas no IgG staining was found in the contralateral side (Fig. 5A). *eSirt6*^{-/-} mice displayed aggravated BBB disruption upon I/R, as confirmed by increased extravasation of IgG as compared to *Sirt6*^{fl/fl} littermates ($d=1.39$ (95%CI 0.35-2.44); $P=0.019$; Fig. 5A).

Brain microvascular endothelial cells constitute the backbone of the BBB structure, their death or apoptosis after I/R injury affects BBB integrity and thus functionality (27, 33). Herein, we co-stained endothelial cells and cleaved

caspase-3 – the common mediator of caspase-dependent apoptotic cascade (34) – in brain slices by immunostaining. Coherently to the higher BBB impairment, *eSirt6*^{-/-} mice also showed increased levels of cleaved-caspase-3 related to endothelial cells in the penumbra area as compared to control littermates suggesting a higher apoptosis rate in response to I/R damage ($d=1.33$ (95%CI 0.59-2.38); $P=0.023$; Fig. 5B).

Impaired barrier function, increased cell death and caspase-3 activation in *SIRT6*-silenced primary HBMVECs after hypoxia/reoxygenation

To test the translational relevance of our *in vivo* findings, primary human brain microvascular endothelial cells (HBMVECs) were exposed to hypoxia for 4 h followed by 4 h of reoxygenation. In line with the observed downregulation of endothelial SIRT6 following I/R in murine cerebral vessels, we observed reduced SIRT6 expression in primary HBMVECs after exposure to hypoxia/reoxygenation ($d=2.51$ (95%CI 1.35-3.67); $P=0.001$; Fig. 6A). To confirm the role of endothelial *SIRT6* in stroke mediated BBB impairment, we assessed the barrier function of *SIRT6*-silenced cells (si*SIRT6*) exposed to hypoxia /reoxygenation (4h/48h, respectively) by using an established *in vitro* BBB model consisting of a monolayer of HBMVECs seeded at confluence in ECIS electrode chambers. *SIRT6* silencing in HBMVECs was achieved by transfection with *SIRT6* siRNA (si*SIRT6*) as compared to siSCR-treated cells ($d=5.77$ (95%CI 4.22-7.32); $P<0.0001$; Fig. 6B). *SIRT6* silencing did not affect cell death rate under normoxic conditions (data not shown). In line with the increased BBB impairment observed in *eSirt6*^{-/-} animals after stroke, si*SIRT6* cells showed lower trans-endothelial resistance compared to siSCR after hypoxia/reperfusion thus suggesting a higher impairment of their barrier function ($P=0.004$; Fig. 6C).

Reflecting the increased endothelial cleaved-caspase 3 expression in cerebral *Sirt6*-deficient vessels after stroke, increased cell death rate and caspase-3 activation was also confirmed in *SIRT6*-silenced HBMVECs exposed to hypoxia/reoxygenation ($d=1.52$ (95%CI 0.43-2.61) and $P=0.015$ for LDH assay and $d=1.32$ (95%CI 0.24-2.40) and $P=0.029$ for caspase 3 activation; Fig. 6D-E). By acting on several downstream targets, Akt pathway is a known regulator of cell survival under stress conditions in different cells, including endothelial ones (35). In line with its critical anti-apoptotic properties, here we report reduced Akt phosphorylation in *SIRT6*-silenced endothelial cells after hypoxia/reoxygenation as compared to siSCR ones ($d= 1.55$ (95%CI 0.46-2.65); $P=0.013$; Fig. 6F). To confirm the involvement of *SIRT6* in the regulation of Akt pathway, we performed a co-immunoprecipitation experiment. First, we found that *SIRT6* co-immunoprecipitates with Akt (Fig. 6G). Furthermore, we observed a reduction of the direct protein-protein interaction after exposure to hypoxia/reoxygenation by approximately 2 fold (Fig. 6G).

Monocyte *SIRT6* gene expression in patients with ischemic stroke correlates with short-term outcome

To substantiate the translational relevance of our data, we analysed *SIRT6* expression levels in monocytes of ischemic stroke patients. In light of the fact that endothelial cells could not be easily obtained, we chose monocytes as a surrogate cell type. A total of 14 ischemic stroke patients were included in the analysis, patients were then divided in those presenting a short-term neurological improvement ($\Delta\text{NIHSS}\%<0$) and those with a worsening of neurologic functions ($\Delta\text{NIHSS}\%>0$). Clinical characteristics of the whole cohort are showed in Table 1. The study sub-groups did not differ significantly in terms of age, sex

distribution, risk factors and comorbidity (Table 1). In ischemic stroke patients, *SIRT6* mRNA levels were significantly higher in patients showing short-term neurological improvement as compared to unfavourable short-term outcome ($d=1.33$ (95%CI 0.25-2.41); $P=0.029$; Fig. 7A). Furthermore, a negative correlation was found between *SIRT6* transcript levels at 24 h from onset of symptoms and the Δ NIHSS% as a measure of short-term neurological outcome ($r=-0.547$ and $P=0.042$; Fig. 7B).

DISCUSSION

Ischemic stroke is an age-related disease with limited treatment options whose incidence is set to increase with the ongoing demographic changes (1, 2, 5). In an effort to deepen our knowledge of the molecular networks underlying age-dependent cardio- and cerebro-vascular disease to identify novel therapeutic target, we previously investigated the role of different aging and longevity genes in the setting of stroke (16, 25, 26, 36). Recently, *SIRT6* has been reported as a longevity gene in mice, primates and humans (37-39). Given the pivotal role of endothelial cells in BBB function and the prognostic relevance of BBB damage in stroke patients, we investigated for the first time the specific function of endothelial *SIRT6* in stroke using animal models, human primary cells and samples from ischemic stroke patients.

In this study, we demonstrate for the first time that endothelial SIRT6 improves outcome after cerebral ischemia/reperfusion injury and that it may represent an interesting novel therapeutic target. Several experimental data substantiate our conclusions: (i) SIRT6 expression is reduced in the murine cerebrovasculature after I/R injury as well as in primary HBMVECs exposed to hypoxia/reoxygenation; (ii) endothelial-specific *Sirt6* genetic deletion increases stroke size and decreases post-stroke survival and neurological deficit by exacerbating apoptosis and BBB dysfunction; (iii) *in vivo* post-ischemic *Sirt6* overexpression blunts stroke-induced cerebral damage and improves outcome; (iv) *SIRT6* silencing impairs barrier function in primary HBMVECs exposed to hypoxia/reoxygenation blunting the activation of Akt salvage pathway and increasing apoptosis rate; (v) *SIRT6* gene expression is increased in ischemic

stroke patients with short-term neurological improvement and correlates with stroke outcome.

A large body of evidence links SIRT6 to longevity as well as to age-dependent disease. SIRT6 prevents premature cell senescence by stabilizing the genome and preserving telomeres (40, 41). In rodents, SIRT6 overexpression increases lifespan while its deletion is associated to premature aging (42-44). Recently, SIRT6 was reported to be protective in endothelial dysfunction, atherosclerosis and cardiac hypertrophy (45-47). Furthermore a protective role for *SIRT6* was also postulated in brain degenerative disease as its expression is reduced in brains of aged animals and Alzheimer's diseases models and, this reduction is associated to neuronal genome instability, cell death, and hyper phosphorylation of tau proteins (48-51). Also, SIRT6 was reported to protect neuronal viability in response to oxygen-glucose deprivation, an *in vitro* model of I/R injury (52, 53). Given the important role of microvascular endothelial cells in BBB function and stroke outcome, in this study we focused on endothelial Sirt6 and found its levels to be reduced in cerebral endothelial cells of brains exposed to I/R and in primary HBMVECs exposed to hypoxia/reoxygenation. These findings suggest that endothelial SIRT6 might be involved in I/R-mediated damage and add novel information to endothelial responses to hypoxic condition. Although, this is in line with previous reports on other cell types (52-55), the exact mechanisms mediating SIRT6 decrease in response to ischemia and hypoxia remain incompletely understood. Hypoxia-inducible factor (HIF)-1 α -mediated downregulation of *SIRT6* expression might be a mediator of SIRT6 decrease since a strong interplay between this transcription factor and *SIRT6* has been previously reported (56, 57).

In our experiments, endothelial *Sirt6* deletion associates with increased cerebral damage and neurological impairment as well as with decreased survival following I/R brain injury, complementing what has been already shown in cardiomyocytes and hepatic cells by other groups (58, 59). Furthermore, our findings are reinforced by the observation that *Sirt6* overexpression reduces brain injury and improves outcome after tMCAO. Of interest in this latter experiment, SIRT6 expression was post-ischemically induced in animals, upon reperfusion so as to mimic the clinical scenario where patients presenting to the emergency room and eligible for reperfusion interventions could be simultaneously treated with additional therapeutic agents. Also, the *Sirt6*-overexpressing construct was administered intravenously and not via intracerebroventricular injection as previously done (52), further endorsing the clinical relevance of our experimental set up.

BBB disruption as a result of I/R damage determines stroke size and associates to worsen clinical outcome. In this study, we could show that endothelial barrier function after ischemia/hypoxia is deeply impaired by SIRT6 depletion both in animals and primary human cells. Indeed, immunohistochemistry analysis of brain slices demonstrates higher extravasation of macromolecules (IgG) -a hallmark of BBB dysfunction- in the ipsilateral hemisphere of eSIRT6^{-/-} animals as compared to control littermates. Mirroring the *in vivo* data, *SIRT6* silencing reduced trans-endothelial resistance -an indicator of barrier function- in our *in vitro* BBB model consisting of primary HBMVECs exposed to hypoxia/reoxygenation. As for mechanisms, our *in vivo* and *in vitro* data consistently point toward an increased apoptosis in endothelial cell exposed to I/R when *SIRT6* is lacking. By co-immunostaining an endothelial marker (CD-31) and cleaved caspase 3 -a key executor in apoptosis- in the penumbra area of infarcted

brains, we showed higher levels of cleaved-caspase 3 related to endothelial cells in *eSirt6*^{-/-} mice after tMCAO as compared to control littermates. While *in vitro*, *SIRT6*-silenced primary HBMVECs show increased death rate and increased cleaved-caspase 3 expression after exposure to hypoxia reoxygenation, as assessed by LDH assay and western blot respectively. The role of SIRT6 in regulation of apoptosis is still matter of debate as both pro- and anti-apoptotic effects have been reported via modulation of different transcription factors (e.g. NF- κ B, HIF1 and c-MYC) (44), particularly SIRT6 effects may depend on the cell type as SIRT6 have been reported to induce apoptosis in cancer cells but not in normal ones (60). Here we found that in HBMVECs exposed to hypoxia/reoxygenation *SIRT6* deletion associates with reduced activation of the Akt salvage pathways, a known negative regulator of apoptosis (35). Also, we report that SIRT6 co-immunoprecipitate with Akt implying a direct protein-protein interaction. Of interest, binding of SIRT6 to Akt was reduced in cells after exposure to hypoxia/reoxygenation. Originally described as a nuclear chromatin-associated deacylase with histone post-translational modification, nowadays SIRT6 is known to localize also in the cytoplasm where it may regulate different pathways (61-63). Of note, previous research demonstrates that the deacetylase function of sirtuins (i.e. SIRT1 and SIRT2) facilitate Akt activation in different cell types (64, 65), this specific effect remains to be investigated for SIRT6 in endothelial cells. Nonetheless, a direct interaction between SIRT6 and Akt was previously shown in embryonic cell lines not exposed to hypoxia/reoxygenation (66).

In order to increase the translational relevance of our preclinical findings, we investigated *SIRT6* expression also in ischemic stroke patients. Here, the isolation of cerebrovascular sample or endothelial cells was not possible thus, monocytes

from whole blood were selected as a surrogate cell type to investigate the relationship between *SIRT6* and stroke outcome. *SIRT6* mRNA levels were increased in ischemic stroke patients showing a short-term neurologic improvement compared to those who showed a worsening. Also, a linear correlation was found between *SIRT6* expression and short term neurologic function. This data are in line with *in vivo* and *in vitro* data herein reported thus supporting the concept of SIRT6 being a positive regulator of stroke outcome.

Some limitations should be taken into consideration when interpreting the herein reported data. First, although we previously demonstrated that *in vivo* cell transfection by mean of cationic reagent (e.g. jetPEI®) primarily targets endothelium in the brain (26), we cannot exclude that other cell types concur to determine the results showed in SIRT6 overexpression experiments. Second, the exact molecular mechanisms linking SIRT6 deficit to blunted activation of Akt salvage pathway following hypoxia/reoxygenation remain unclear. However, a direct deacetylase function of SIRT6 on Akt is a likely mechanism in this case. Finally, monocytes were chosen as surrogate cells for studying *SIRT6* expression in ischemic stroke patients given the difficulty of obtaining cerebrovascular specimens. Clearly, results from this proof of principle experiment are purely associative and will require additional confirmatory investigations aiming at assessing the cause and effect relationship thus supporting our conclusions regarding their possible clinical applications.

CONCLUSIONS

In conclusion, this translational study indicates that endothelial SIRT6 exerts a beneficial role in cerebral ischemia/reperfusion injury by preserving blood-brain barrier integrity. At the molecular level, SIRT6 might modulate I/R-induced apoptosis by reducing caspase-3 activation through the Akt salvage pathways. Data from this study set the stage for further investigation to validate endothelial SIRT6 as a novel therapeutic target for the treatment of ischemic stroke.

TABLES AND FIGURES

Table 1. Characteristics of the study population.

	Study population (n=14)	Δ NIHSS%<0 (n=7)	Δ NIHSS%>0 (n=7)	p- value
Demographic, risk factors and comorbidities				
Age, years (range)	73.3 (54-90)	68.0 (57-90)	78.6 (70-85)	0.053
Female, n (%)	6 (42.9%)	2 (28.6%)	4 (57.1%)	0.280
Smoking, n (%)	5 (35.7%)	3 (42.9%)	2 (28.6%)	0.593
Hypertension, n (%)	8 (57.1%)	3 (42.9%)	4 (57.1%)	0.577
Dyslipidemia, n (%)	1 (7.1%)	1 (14.3%)	0 (0%)	0.299
Diabetes, n (%)	0 (0%)	0 (0%)	0 (0%)	1.000
Coronary artery disease, n (%)	3 (21.4%)	2 (28.6%)	1 (14.3%)	0.515
Previous TIA/stroke, n (%)	1 (7.1%)	1 (14.3%)	0 (0%)	0.299
Peripheral artery disease, n (%)	4 (28.6%)	2 (28.6%)	2 (28.6%)	1.000
Thrombolysis, n (%)	5 (35.7%)	3 (42.9%)	2 (28.6%)	0.593
TOAST classification				
Large vessel atherosclerosis, n (%)	3 (21.4%)	1 (14.3%)	2 (14.3%)	0.515
Cardioembolism, n (%)	7 (50%)	3 (42.9%)	4 (57.1%)	0.577
Small vessel disease, n (%)	1 (7.1%)	1 (14.3%)	0 (0%)	0.299
Undetermined cause, n (%)	1 (7.1%)	1 (14.3%)	0 (0%)	0.299
Other cause, n (%)	2 (14.3%)	1 (14.3%) [#]	1 (14.3%) [*]	1.000
Stroke assessment				
NIHSS admission, mean (SD)	10.6 (5.6)	8.9 (5.0)	12.4 (6.5)	0.383
NIHSS discharge, mean (SD)	10.6 (10.3)	3.3 (2.3)	18.0 (10.8)	0.007
Stroke size, mL (SD)	40.1 (59.5)	17.4 (18.2)	62.7 (78.4)	0.535
MCA occlusion, n (%)	7 (50.0%)	4 (57.1%)	3 (42.9%)	0.577
Early complications				
Haemorrhagic transformation, n (%)	0 (0%)	0 (0%)	0 (0%)	1.000
Cerebral edema, n (%)	3 (21.4%)	0 (0%)	3 (42.9%)	0.051

TIA = Transient Ischemic Attack.
NIHSS = National Institute of Health Stroke Scale
MCA = Middle Cerebral Artery
Embolism due to endovascular procedure
* Hypercoagulability

Figure 1

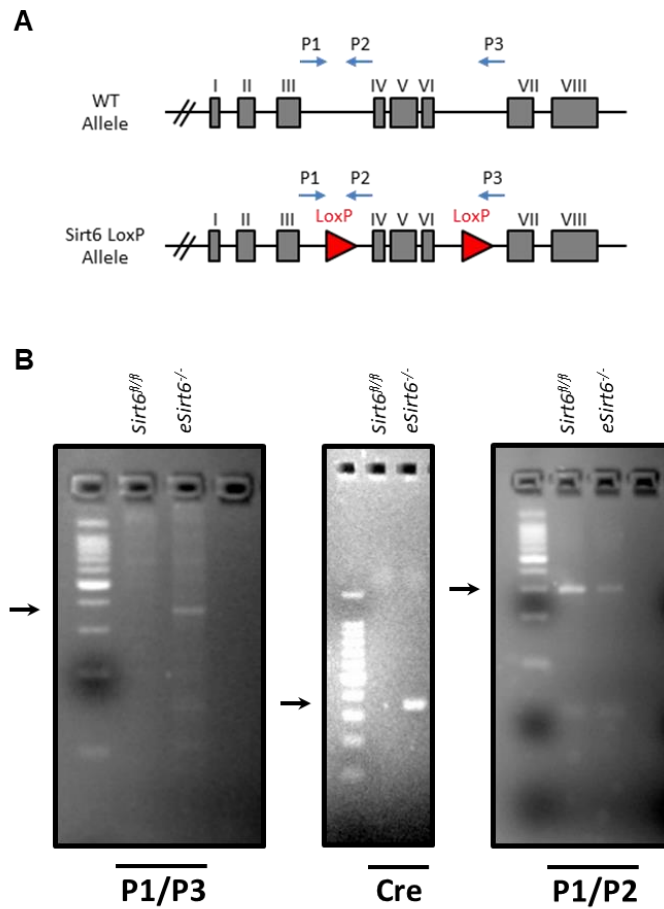


Figure 1. Generation and characterization of endothelial-specific SIRT6 knock out mice (A) Schematic representation of the targeting strategy for the genetic deletion of *Sirt6* gene. (B) Genomic PCR on endothelial cells isolated from either endothelial-specific *Sirt6* homozygous knockout mice (*eSirt6^{-/-}*) or corresponding controls (*Sirt6^{fl/fl}*) using *Sirt6*-specific primers *P1* and *P3* (left panel), *Cre*-specific primers (middle panel) or *Sirt6*-specific primers *P1* and *P2* (right panel). The position of the corresponding PCR product is shown by arrows. (C-G) Circulating levels of total cholesterol, low-density lipoprotein cholesterol, high-density lipoprotein cholesterol, triglycerides and glucose did not differ between *eSirt6^{-/-}* and *Sirt6^{fl/fl}* (n=5).

Figure 2

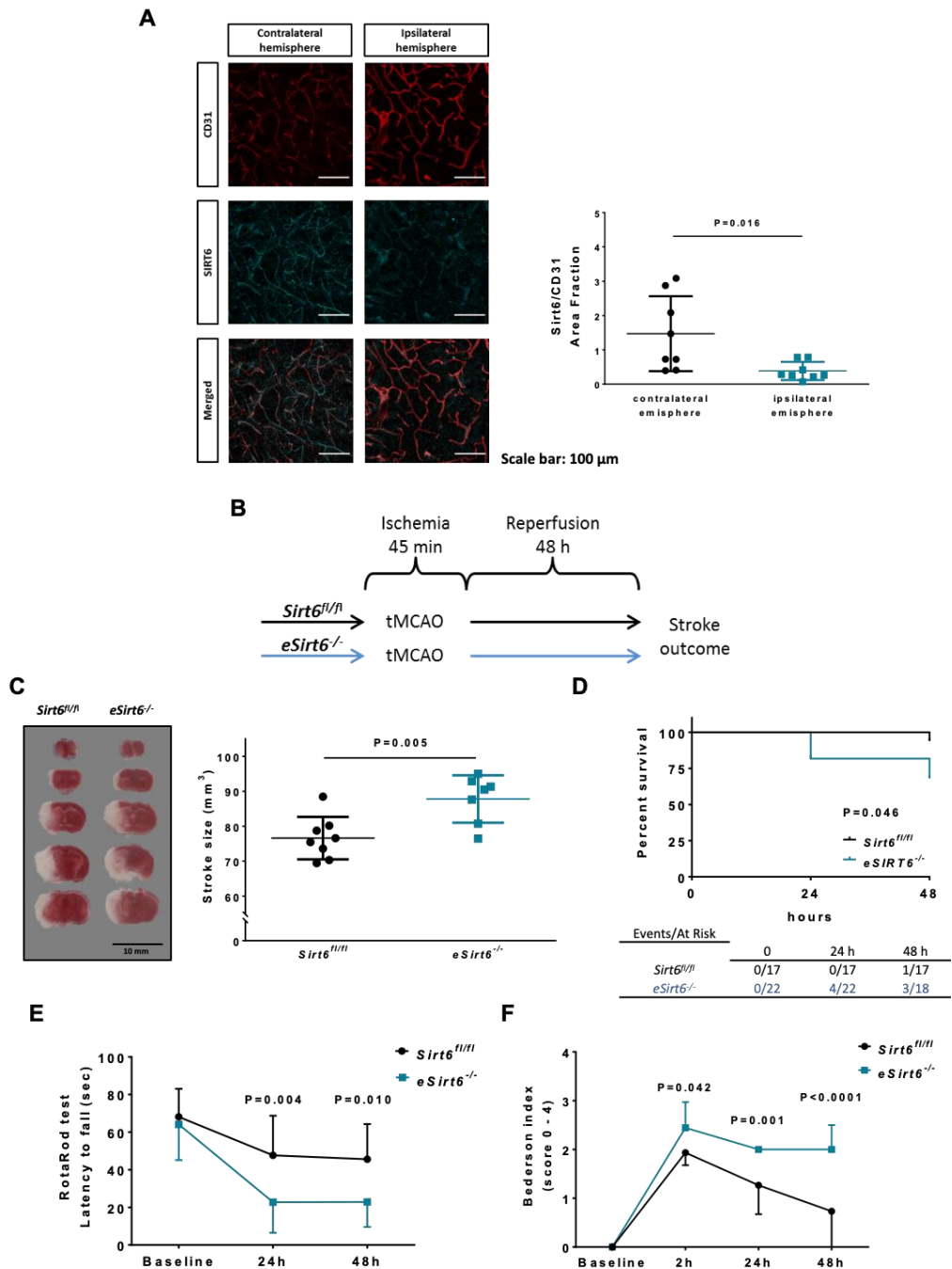


Figure 2. Impact of endothelial Sirt6 deletion on cerebral lesion, survival and neurological deficit after tMCAO in mice. (A) After tMCAO, SIRT6 expression (red) relative to endothelial cells (cyan for CD31) is reduced in vessel located in the ipsilateral hemisphere as compared to the contralateral ones (representative images and quantification; n=8). (B) Schematic of experimental set up. (C) *eSirt6^{-/-}* mice showed increased stroke volumes (representative pictures and quantification; n=7-8), (D) reduced survival at 48 h (n=17-22) and decreased neurological functions as assessed by (E) RotaRod or (F) Bederson-based neurological score (n=17-22), as compared to *Sirt6^{fl/fl}* littermates. CD: cluster of differentiation; *eSirt6^{-/-}*=endothelial-specific Sirt6 knock out animals; *SIRT6^{fl/fl}*=Sirt6-floxed control animals; tMCAO=transient middle cerebral artery occlusion.

Figure 3

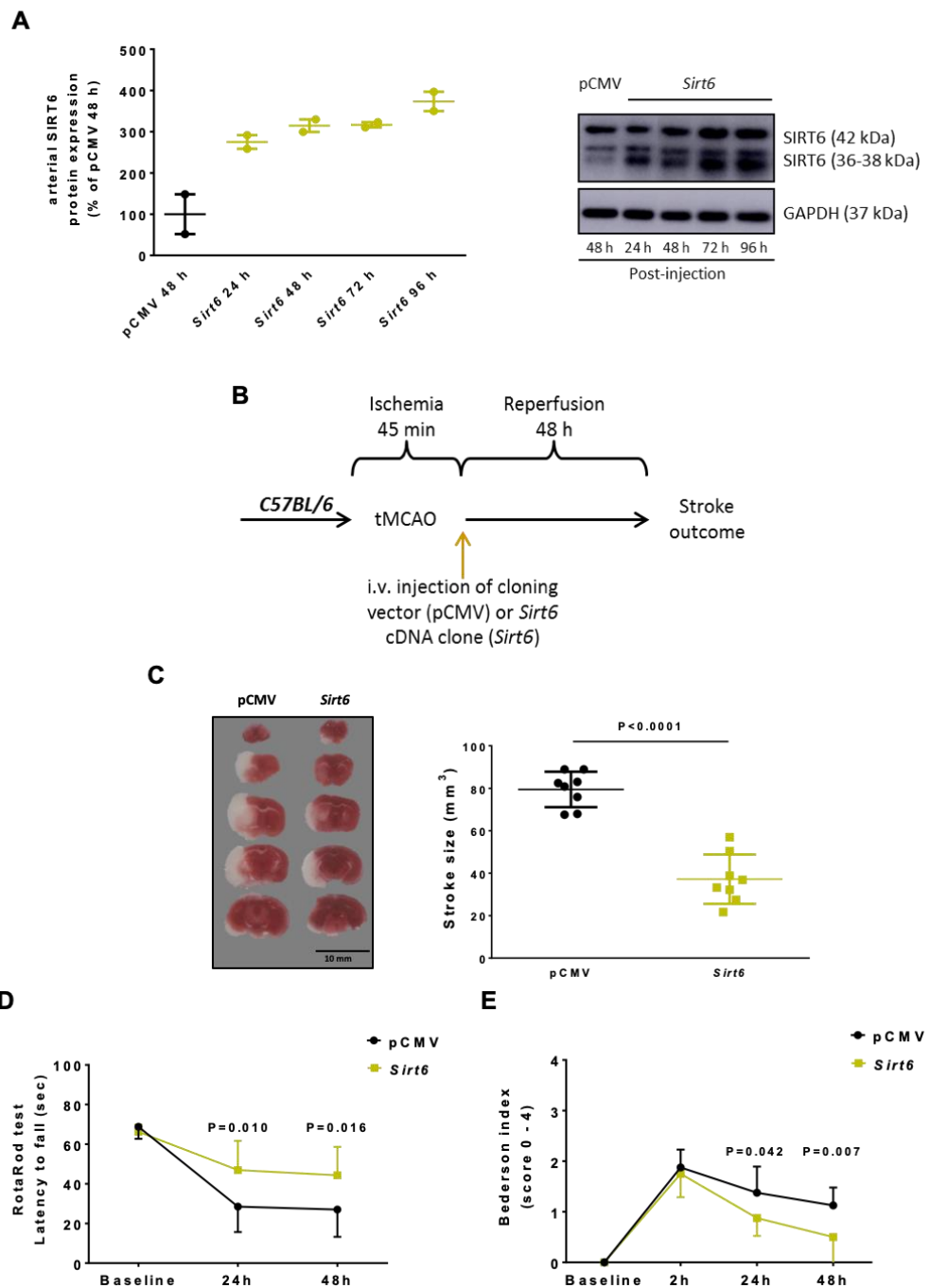


Figure 3. Effects of post-ischemic Sirt6 overexpression on cerebral damage and neurological deficit after tMCAO. (A) Arterial SIRT6 expression is increased by about 3 folds 24 h after the injection of Sirt6 construct (Sirt6), as compared to animals treated with control construct (pCMV) (quantification and representative blot; n=2). (B) Schematic of clinically relevant experimental set up in which the expression of Sirt6 have been induced in WT C57BL/6 animals vivo at the beginning of the reperfusion. (C) Post-ischemic administration of the Sirt6 construct decreases stroke volume 48 h after tMCAO (representative pictures and quantification) and blunted neurological deficit as assessed by (D) RotaRod and (E) Bederson-based neurological scale, as compared to animals treated with control construct (pCMV) (n=8 for all). GAPDH=glyceraldehyde 3-phosphate dehydrogenase; tMCAO=temporary middle cerebral artery occlusion.

Figure 4

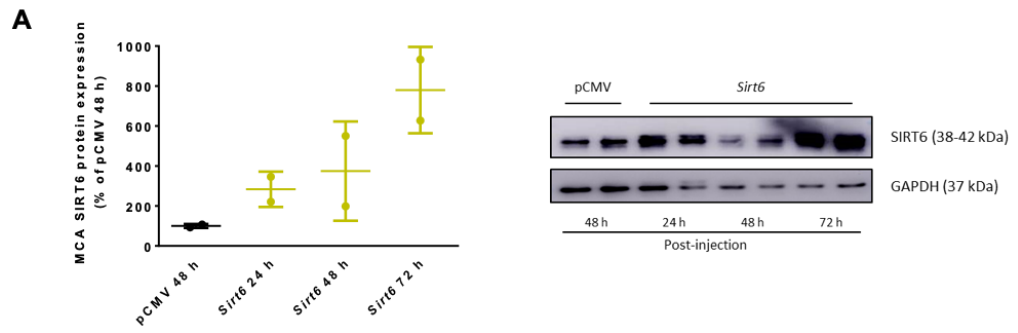
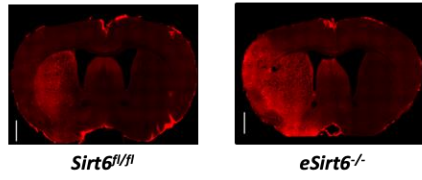


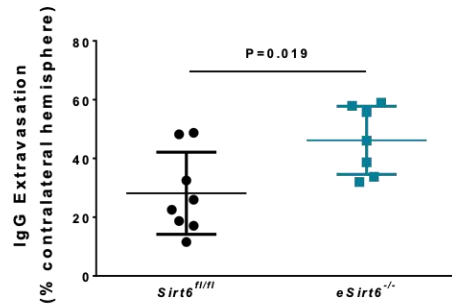
Figure 4. SIRT6 cDNA delivery to middle cerebral arteries (MCAs) (A) MCA SIRT6 expression is increased by about 3 folds 24 h after the injection of Sirt6 construct (Sirt6), as compared to animals treated with control construct (pCMV) (quantification and blot; n=2).

Figure 5

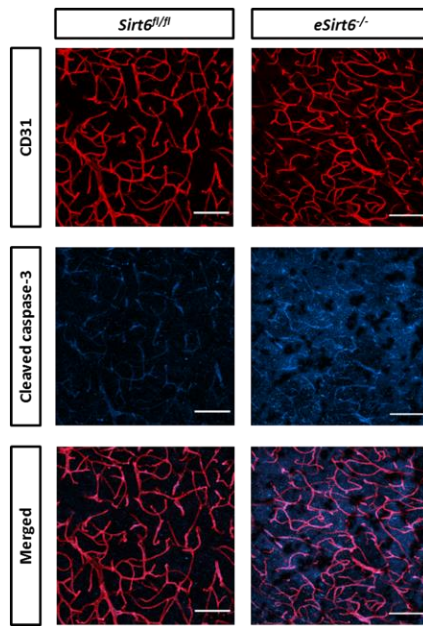
A



Scale bar: 1000 μ m



B



Scale bar: 100 μ m

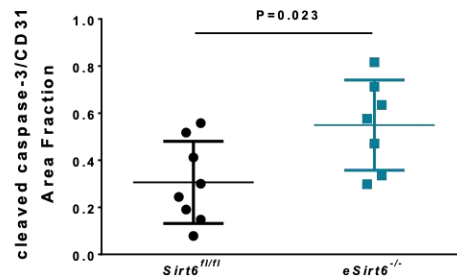


Figure 5. Impact of endothelial *Sirt6* deletion on BBB damage and endothelial apoptosis after tMCAO. (A) At 48 h after stroke *eSirt6*^{-/-} animals showed increased IgG extravasation (red) in the ipsilateral hemisphere denoting a higher BBB impairment, as compared to control littermates (*SIRT6*^{fl/fl}) (representative picture of immunostaining and quantification; n=7-8). (B) After stroke, cleaved caspase-3 (cyan) expression relative to endothelial cells (red for CD31) is increased in the penumbra area of *eSirt6*^{-/-} animals, as compared to *Sirt6*^{fl/fl} control littermates (representative picture of immunostaining and quantification; n=7-8). CD= cluster of differentiation; *eSirt6*^{-/-}=endothelial-specific *Sirt6* knock out animals; IgG= immunoglobulin G; *SIRT6*^{fl/fl}=*Sirt6*-floxed control animals; tMCAO=transient middle cerebral artery occlusion.

Figure 6

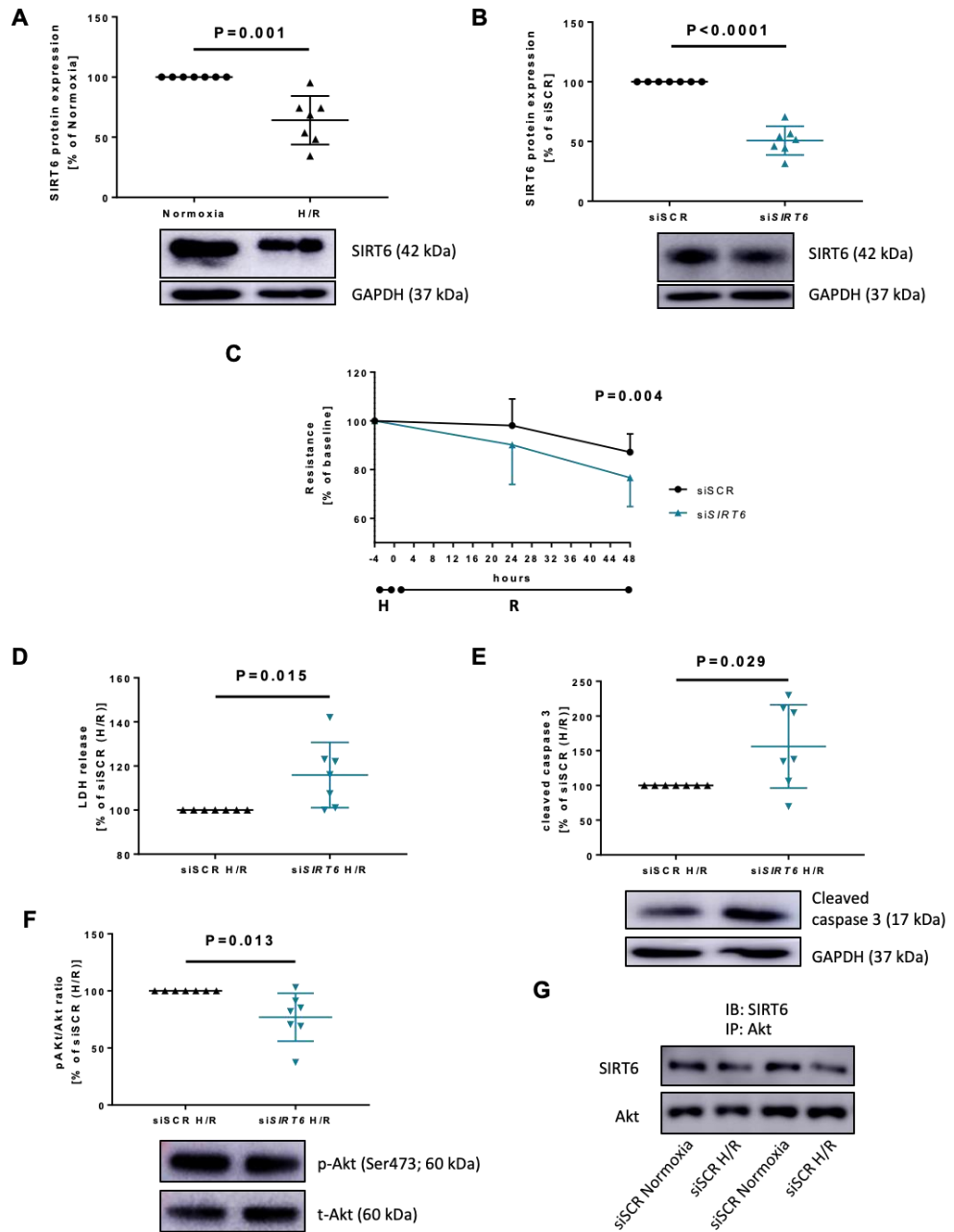


Figure 6. SIRT6 responsiveness and effects of SIRT6 silencing on barrier function, cell death and apoptosis in primary HBMVECs after hypoxia/reoxygenation. (A) SIRT6 expression is reduced in primary HBMVECs after exposure to hypoxia/reoxygenation (4 h/4 h), as compared with normoxia (8 h) (n=7). (B) In HBMVECs, SIRT6 protein expression (n=7) is significantly reduced after transfection with SIRT6 small interfering RNA (siSIRT6) as compared to control siRNA (siSCR) (n=7). (C) SIRT6 silencing reduces endothelial barrier function as assessed by continuous trans-endothelial resistance measurement (n=11). (D) Endothelial cell death in siSIRT6-transfected HBMVECs was increased, compared with siSCR-treated cells after exposure to hypoxia/reoxygenation (n=7). (E) Activated (cleaved) caspase-3 protein expression was upregulated in SIRT6-transfected HBMVECs, compared with siSCR-transfected ones after exposure to hypoxia/reoxygenation (n=7). (F) siSIRT6-treated cells showed reduced activation of the Akt salvage pathway (n=7). (G) Representative immunoblot of co-immunoprecipitation of Akt and SIRT6 from whole-cell lysates of siSCR-treated cells under normoxic conditions and after H/R. GAPDH=glyceraldehyde 3-phosphate

dehydrogenase, H/R=hypoxia/reoxygenation, HBMVECs=human brain microvascular endothelial cells, IP: immunoprecipitation; IB=immunoblot; LDH = lactate dehydrogenase.

Figure 7

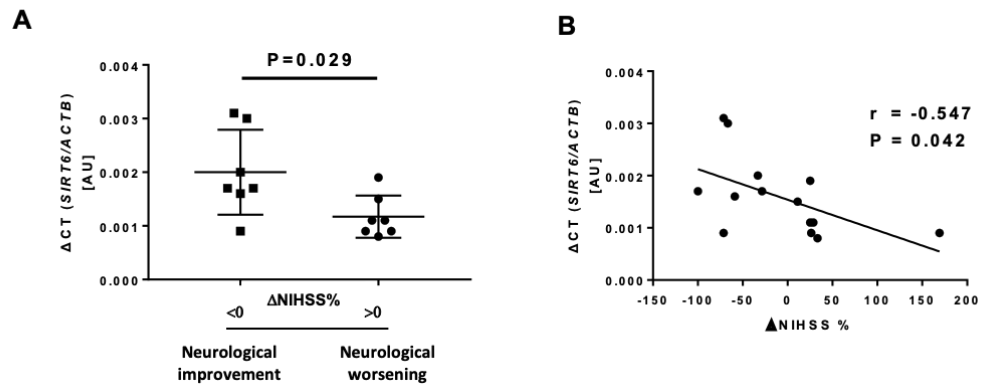


Figure 7. SIRT6 gene expression in patients with ischemic stroke and its correlations with the short-term outcome. (A) Monocyte SIRT6 mRNA expression is increased in ischemic stroke patients showing short-term neurological improvement (Δ NIHSS% <0) as compared to those with worse outcome (Δ NIHSS% >0) (n=14). (B) In ischemic stroke patients there is a linear correlation between SIRT6 transcript levels and short-term neurological outcome as assessed by the neurological deficit assessed by the National Institute of Health Stroke Scale (NIHSS) (n=14). ACTB=beta actin protein.

REFERENCES

1. Camici GG, Liberale L. Aging: the next cardiovascular disease? *Eur Heart J.* 2017;38(21):1621-3.
2. Liberale L, Carbone F, Montecucco F, Gebhard C, Luscher TF, Wegener S, et al. Ischemic stroke across sexes: What is the status quo? *Front Neuroendocrin.* 2018;50:3-17.
3. Granger DN, Kvietys PR. Reperfusion injury and reactive oxygen species: The evolution of a concept. *Redox Biol.* 2015;6:524-51.
4. Powers WJ, Rabinstein AA, Ackerson T, Adeoye OM, Bambakidis NC, Becker K, et al. 2018 Guidelines for the Early Management of Patients With Acute Ischemic Stroke: A Guideline for Healthcare Professionals From the American Heart Association/American Stroke Association. *Stroke; a journal of cerebral circulation.* 2018;49(3):E46-E110.
5. Bonaventura A, Liberale L, Vecchie A, Casula M, Carbone F, Dallegri F, et al. Update on Inflammatory Biomarkers and Treatments in Ischemic Stroke. *Int J Mol Sci.* 2016;17(12).
6. Widimsky P, Coram R, Abou-Chebl A. Reperfusion therapy of acute ischaemic stroke and acute myocardial infarction: similarities and differences. *Eur Heart J.* 2014;35(3):147-+.
7. Molina CA. Reperfusion Therapies for Acute Ischemic Stroke Current Pharmacological and Mechanical Approaches. *Stroke; a journal of cerebral circulation.* 2011;42(1):S16-S9.
8. Fu Y, Liu Q, Anrather J, Shi FD. Immune interventions in stroke. *Nat Rev Neurol.* 2015;11(9):524-35.

9. Bonaventura A, Montecucco F, Dallegri F, Carbone F, Luscher TF, Camici GG, et al. Novel findings in neutrophil biology and their impact on cardiovascular disease. *Cardiovasc Res*. 2019.
10. d'Este CD, Fainardi E, Aviv RI, Lee TY. Improving Acute Stroke Management with Computed Tomography Perfusion: A Review of Imaging Basics and Applications. *Transl Stroke Res*. 2012;3(2):205-20.
11. Scalzo F, Alger JR, Hu X, Saver JL, Dani KA, Muir KW, et al. Multi-center prediction of hemorrhagic transformation in acute ischemic stroke using permeability imaging features. *Magn Reson Imaging*. 2013;31(6):961-9.
12. Mardor Y, Tanne D, Daniels D, Last D, Shneur R, Guez D, et al. The Application of MRI for Depiction of Blood Brain Barrier Opening in Stroke. *Stroke; a journal of cerebral circulation*. 2010;41(4):E338-E.
13. Paneni F, Canestro CD, Libby P, Luscher TF, Camici GG. The Aging Cardiovascular System Understanding It at the Cellular and Clinical Levels. *Journal of the American College of Cardiology*. 2017;69(15):1952-67.
14. Camici GG, Savarese G, Akhmedov A, Luscher TF. Molecular mechanism of endothelial and vascular aging: implications for cardiovascular disease. *Eur Heart J*. 2015;36(48):3392-U109.
15. Satoh A, Imai S, Guarente L. The brain, sirtuins, and ageing. *Nat Rev Neurosci*. 2017;18(6):362-74.
16. Diaz-Canestro C, Merlini M, Bonetti NR, Liberale L, Wust P, Briand-Schumacher S, et al. Sirtuin 5 as a novel target to blunt blood-brain barrier damage induced by cerebral ischemia/reperfusion injury. *Int J Cardiol*. 2018;260:148-55.

17. Winnik S, Auwerx J, Sinclair DA, Matter CM. Protective effects of sirtuins in cardiovascular diseases: from bench to bedside. *Eur Heart J.* 2015;36(48):3404-12.
18. Tang BL. Is SIRT6 Activity Neuroprotective and How Does It Differ from SIRT1 in This Regard? *Front Cell Neurosci.* 2017;11.
19. Zhang W, Wei R, Zhang L, Tan Y, Qian CY. Sirtuin 6 Protects the Brain from Cerebral Ischemia/Reperfusion Injury through Nrf2 Activation. *Neuroscience.* 2017;366:95-104.
20. Paneni F, Osto E, Costantino S, Mateescu B, Briand S, Coppolino G, et al. Deletion of the Activated Protein-1 Transcription Factor JunD Induces Oxidative Stress and Accelerates Age-Related Endothelial Dysfunction. *Circulation.* 2013;127(11):1229-+.
21. van Beijnum JR, Rousch M, Castermans K, van der Linden E, Griffioen AW. Isolation of endothelial cells from fresh tissues. *Nat Protoc.* 2008;3(6):1085-91.
22. Liberale L, Diaz-Canestro C, Bonetti NR, Paneni F, Akhmedov A, Beer JH, et al. Post-ischaemic administration of the murine Canakinumab-surrogate antibody improves outcome in experimental stroke. *Eur Heart J.* 2018;39(38):3511-7.
23. Bonetti NR, Diaz-Canestro C, Liberale L, Crucet M, Akhmedov A, Merlini M, et al. Tumour Necrosis Factor-alpha Inhibition Improves Stroke Outcome in a Mouse Model of Rheumatoid Arthritis. *Sci Rep.* 2019;9(1):2173.
24. Bederson JB, Pitts LH, Tsuji M, Nishimura MC, Davis RL, Bartkowski H. Rat middle cerebral artery occlusion: evaluation of the model and development of a neurologic examination. *Stroke; a journal of cerebral circulation.* 1986;17(3):472-6.

25. Diaz-Canestro C, Reiner MF, Bonetti NR, Liberale L, Merlini M, Wust P, et al. AP-1 (Activated Protein-1) Transcription Factor JunD Regulates Ischemia/Reperfusion Brain Damage via IL-1beta (Interleukin-1beta). *Stroke; a journal of cerebral circulation*. 2019;50(2):469-77.
26. Spescha RD, Klohs J, Semerano A, Giacalone G, Derungs RS, Reiner MF, et al. Post-ischaemic silencing of p66Shc reduces ischaemia/reperfusion brain injury and its expression correlates to clinical outcome in stroke. *Eur Heart J*. 2015;36(25):1590-600.
27. Akhmedov A, Bonetti NR, Reiner MF, Spescha RD, Amstalden H, Merlini M, et al. Deleterious role of endothelial lectin-like oxidized low-density lipoprotein receptor-1 in ischaemia/reperfusion cerebral injury. *J Cereb Blood Flow Metab*. 2018:271678X18793266.
28. Adams HP, Jr., Bendixen BH, Kappelle LJ, Biller J, Love BB, Gordon DL, et al. Classification of subtype of acute ischemic stroke. Definitions for use in a multicenter clinical trial. TOAST. Trial of Org 10172 in Acute Stroke Treatment. *Stroke; a journal of cerebral circulation*. 1993;24(1):35-41.
29. Mair G, von Kummer R, Morris Z, von Heijne A, Bradey N, Cala L, et al. Effect of alteplase on the CT hyperdense artery sign and outcome after ischemic stroke. *Neurology*. 2016;86(2):118-25.
30. Sims JR, Gharai LR, Schaefer PW, Vangel M, Rosenthal ES, Lev MH, et al. ABC/2 for rapid clinical estimate of infarct, perfusion, and mismatch volumes. *Neurology*. 2009;72(24):2104-10.
31. Franzeck FC, Hof D, Spescha RD, Hasun M, Akhmedov A, Steffel J, et al. Expression of the aging gene p66Shc is increased in peripheral blood monocytes of patients with acute coronary syndrome but not with stable coronary artery disease. *Atherosclerosis*. 2012;220(1):282-6.

32. Hedges LV, Pigott TD. The power of statistical tests in meta-analysis. *Psychol Methods*. 2001;6(3):203-17.
33. Zhang Y, Wang T, Yang K, Xu J, Ren L, Li W, et al. Cerebral Microvascular Endothelial Cell Apoptosis after Ischemia: Role of Enolase-Phosphatase 1 Activation and Aci-Reductone Dioxygenase 1 Translocation. *Front Mol Neurosci*. 2016;9:79.
34. Li J, Yuan J. Caspases in apoptosis and beyond. *Oncogene*. 2008;27(48):6194-206.
35. Franke TF, Hornik CP, Segev L, Shostak GA, Sugimoto C. PI3K/Akt and apoptosis: size matters. *Oncogene*. 2003;22(56):8983-98.
36. Spescha RD, Shi Y, Wegener S, Keller S, Weber B, Wyss MM, et al. Deletion of the ageing gene p66(Shc) reduces early stroke size following ischaemia/reperfusion brain injury. *Eur Heart J*. 2013;34(2):96-103.
37. Zhang W, Wan H, Feng G, Qu J, Wang J, Jing Y, et al. SIRT6 deficiency results in developmental retardation in cynomolgus monkeys. *Nature*. 2018;560(7720):661-5.
38. Kanfi Y, Naiman S, Amir G, Peshti V, Zinman G, Nahum L, et al. The sirtuin SIRT6 regulates lifespan in male mice. *Nature*. 2012;483(7388):218-21.
39. Hirvonen K, Laivuori H, Lahti J, Strandberg T, Eriksson JG, Hackman P. SIRT6 polymorphism rs117385980 is associated with longevity and healthy aging in Finnish men. *BMC Med Genet*. 2017;18(1):41.
40. Jia G, Su L, Singhal S, Liu X. Emerging roles of SIRT6 on telomere maintenance, DNA repair, metabolism and mammalian aging. *Mol Cell Biochem*. 2012;364(1-2):345-50.
41. Liao CY, Kennedy BK. SIRT6, oxidative stress, and aging. *Cell Res*. 2016;26(2):143-4.

42. Roichman A, Kanfi Y, Glazz R, Naiman S, Amit U, Landa N, et al. SIRT6 Overexpression Improves Various Aspects of Mouse Healthspan. *J Gerontol A Biol Sci Med Sci.* 2017;72(5):603-15.
43. Peshti V, Obolensky A, Nahum L, Kanfi Y, Rathaus M, Avraham M, et al. Characterization of physiological defects in adult SIRT6^{-/-} mice. *PLoS One.* 2017;12(4):e0176371.
44. Tasselli L, Zheng W, Chua KF. SIRT6: Novel Mechanisms and Links to Aging and Disease. *Trends Endocrinol Metab.* 2017;28(3):168-85.
45. Xu S, Yin M, Koroleva M, Mastrangelo MA, Zhang W, Bai P, et al. SIRT6 protects against endothelial dysfunction and atherosclerosis in mice. *Aging (Albany NY).* 2016;8(5):1064-82.
46. Balestrieri ML, Rizzo MR, Barbieri M, Paolisso P, D'Onofrio N, Giovane A, et al. Sirtuin 6 expression and inflammatory activity in diabetic atherosclerotic plaques: effects of incretin treatment. *Diabetes.* 2015;64(4):1395-406.
47. Pillai VB, Sundaresan NR, Gupta MP. Regulation of Akt signaling by sirtuins: its implication in cardiac hypertrophy and aging. *Circ Res.* 2014;114(2):368-78.
48. Jesko H, Wencel P, Strosznajder RP, Strosznajder JB. Sirtuins and Their Roles in Brain Aging and Neurodegenerative Disorders. *Neurochem Res.* 2017;42(3):876-90.
49. Braidy N, Poljak A, Grant R, Jayasena T, Mansour H, Chan-Ling T, et al. Differential expression of sirtuins in the aging rat brain. *Front Cell Neurosci.* 2015;9:167.
50. Jung ES, Choi H, Song H, Hwang YJ, Kim A, Ryu H, et al. p53-dependent SIRT6 expression protects Abeta42-induced DNA damage. *Sci Rep.* 2016;6:25628.

51. Kaluski S, Portillo M, Besnard A, Stein D, Einav M, Zhong L, et al. Neuroprotective Functions for the Histone Deacetylase SIRT6. *Cell Rep.* 2017;18(13):3052-62.
52. Zhang W, Wei R, Zhang L, Tan Y, Qian C. Sirtuin 6 protects the brain from cerebral ischemia/reperfusion injury through NRF2 activation. *Neuroscience.* 2017;366:95-104.
53. Lee OH, Kim J, Kim JM, Lee H, Kim EH, Bae SK, et al. Decreased expression of sirtuin 6 is associated with release of high mobility group box-1 after cerebral ischemia. *Biochem Biophys Res Commun.* 2013;438(2):388-94.
54. Mao Z, Tian X, Van Meter M, Ke Z, Gorbunova V, Seluanov A. Sirtuin 6 (SIRT6) rescues the decline of homologous recombination repair during replicative senescence. *Proc Natl Acad Sci U S A.* 2012;109(29):11800-5.
55. Van Meter M, Kashyap M, Rezazadeh S, Geneva AJ, Morello TD, Seluanov A, et al. SIRT6 represses LINE1 retrotransposons by ribosylating KAP1 but this repression fails with stress and age. *Nat Commun.* 2014;5:5011.
56. Zhong L, D'Urso A, Toiber D, Sebastian C, Henry RE, Vadysirisack DD, et al. The histone deacetylase Sirt6 regulates glucose homeostasis via Hif1alpha. *Cell.* 2010;140(2):280-93.
57. Zwaans BM, Lombard DB. Interplay between sirtuins, MYC and hypoxia-inducible factor in cancer-associated metabolic reprogramming. *Dis Model Mech.* 2014;7(9):1023-32.
58. Zhang S, Jiang S, Wang H, Di W, Deng C, Jin Z, et al. SIRT6 protects against hepatic ischemia/reperfusion injury by inhibiting apoptosis and autophagy related cell death. *Free Radic Biol Med.* 2018;115:18-30.
59. Wang XX, Wang XL, Tong MM, Gan L, Chen H, Wu SS, et al. SIRT6 protects cardiomyocytes against ischemia/reperfusion injury by augmenting

FoxO3alpha-dependent antioxidant defense mechanisms. *Basic Res Cardiol.* 2016;111(2):13.

60. Van Meter M, Mao Z, Gorbunova V, Seluanov A. SIRT6 overexpression induces massive apoptosis in cancer cells but not in normal cells. *Cell Cycle.* 2011;10(18):3153-8.

61. Ardestani PM, Liang F. Sub-cellular localization, expression and functions of Sirt6 during the cell cycle in HeLa cells. *Nucleus.* 2012;3(5):442-51.

62. Simeoni F, Tasselli L, Tanaka S, Villanova L, Hayashi M, Kubota K, et al. Proteomic analysis of the SIRT6 interactome: novel links to genome maintenance and cellular stress signaling. *Sci Rep.* 2013;3:3085.

63. Jedrusik-Bode M, Studencka M, Smolka C, Baumann T, Schmidt H, Kampf J, et al. The sirtuin SIRT6 regulates stress granule formation in *C. elegans* and mammals. *J Cell Sci.* 2013;126(Pt 22):5166-77.

64. Ramakrishnan G, Davaakhuu G, Kaplun L, Chung WC, Rana A, Atfi A, et al. Sirt2 deacetylase is a novel AKT binding partner critical for AKT activation by insulin. *The Journal of biological chemistry.* 2014;289(9):6054-66.

65. Sundaresan NR, Pillai VB, Wolfgeher D, Samant S, Vasudevan P, Parekh V, et al. The deacetylase SIRT1 promotes membrane localization and activation of Akt and PDK1 during tumorigenesis and cardiac hypertrophy. *Sci Signal.* 2011;4(182):ra46.

66. Thirumurthi U, Shen J, Xia W, LaBaff AM, Wei Y, Li CW, et al. MDM2-mediated degradation of SIRT6 phosphorylated by AKT1 promotes tumorigenesis and trastuzumab resistance in breast cancer. *Sci Signal.* 2014;7(336):ra71.

ACKNOWLEDGEMENTS

To my whole family. My wife Marta, for all the love, enthusiasm and moral support she has provided me in front of every success or defeat of this long road. My parents, Nonna Anna, Michela and Pier Paolo deserve special thanks for their never-ending support and encouragement. How not to mention my nephews Ettore and Leonardo for helping me to unplug and recharge from the stress during my weekends home. Without such a team behind me, I doubt that I would be in this place today.

A very special gratitude to Profs. Montecucco and Camici, for their fundamental mentoring, their contributions to my professional training and the opportunities they gave to me during these years.

I am also grateful to all collaborators in this PhD projects for their fundamental contributions and for helping and providing solutions to all my doubts.

Staying at the Center for Molecular Cardiology during these years has been amazing. For their friendship and never-ending support, I particularly want to thank Prof. Luscher, Alexander, Lena, Vanasa, Nicole, Ana, Yustina, Shafeeq, Samuele, Stephan, Sara and Simon.

Finally, I am also grateful to Aldo and Alessandra for taking time for our overseas videocall during which we shared achievements and fears. A special mention also to Federico for always being supportive and keen to help.

Thanks for all your encouragement!